Are estimates of anthropogenic and natural influences on Australia's extreme 2010-2012 rainfall model-dependent?

Sophie C. Lewis[a*], David J. Karoly[a]

[a] School of Earth Sciences and ARC Centre of Excellence for Climate System Science, University of Melbourne, Melbourne, Victoria, 3010, Australia

[*] Corresponding author: Tel: +61 3 8344 6907; email: sophie.lewis@unimelb.edu.au

Abstract

Australia experienced much above average rainfall in association with strong, extended La Niña conditions during 2010-2012. Was the heavy Australian rainfall influenced by La Niña conditions and/or anthropogenic greenhouse gases? We investigate the relative contributions of anthropogenic climate change and natural climatic variability to the likelihood of heavy Australian rainfall using three distinct model datasets. Area-average rainfall anomalies for model simulations with natural forcings only were compared to simulations with both anthropogenic and natural forcings using 16 models participating in the Coupled Model Intercomparison Project Phase 5 (CMIP5). Using fraction of attributable risk to compare the likelihood of unusual rainfall between the parallel experiments, we find attribution statements are uncertain, with FAR values sensitive to the attribution parameters considered, including thresholds, regions and seasons. When heavy rainfall probabilities were next investigated in ensembles of two atmospheric general circulation models, run with and without anthropogenically-induced sea surface temperature changes, results were model-dependent. Overall, the attribution of seasonal-scale heavy Australia rainfall to a particular cause is likely more complicated than for temperature extremes. As estimates of the greenhouse gas attributable change in rainfall risk may depend on the model datasets considered, it is also useful to consider model outputs from several datasets and using various estimates of counterfactual surface conditions to establish robust attribution statements for extreme rainfall events. In contrast, comparing the likelihoods of heavy rainfall during simulated La Niña years with El Niño/neutral years reveals a substantial La Niña influence on Australian rainfall during 2010-2012 that is robust to changes in the attribution framework.

Keywords

Attribution; climate change; extreme rainfall; ENSO; Australia

1. Introduction

Eastern Australia experienced extreme precipitation in 2010-2012: rainfall records were broken on daily through to seasonal timescales for large regions [*Bureau of Meteorology*, 2012a; 2012b; *Ganter and Tobin*, 2013]. Persistent, heavy rainfall ended the drought of the preceding decade, but resulted in severe flooding and billions of dollars of flood damage occurred in northern Australia, leading to the evacuation of thousands and 35 deaths. Furthermore, wet conditions were contemporaneous with two strong, consecutive La Niña events, which are typically associated with enhanced eastern Australian rainfall.

The coincidence of the strong La Niña and heavy Australian rainfall prompted suggestions that La Niña conditions were responsible for the extreme Australian rainfall [*Nicholls*, 2011]. However, the amount of Australian rainfall typically associated with El Niño-Southern Oscillation (ENSO) conditions is not temporally stationary [*Nicholls et al.*, 1996] and may be also affected by longer term anthropogenic warming trends [*Li et al.*, 2013]. Observed high local sea surface temperatures (SSTs) around northern Australia observed during 2010-2011 were also potentially influential on the extreme rainfall occurring during this time [*Evans and Boyer-Souchet*, 2012]. Unusual ocean temperatures may also have been a result of the longer-term anthropogenic-warming signal.

Was the heavy Australian rainfall influenced by La Niña conditions and/or climate change due to increasing greenhouse gases (GHGs)? Disentangling the multiple possible influences on the 2010-2012 rainfall extremes in a quantitative manner provides a challenging scientific problem. Previous studies have partly addressed questions around anthropogenic influences on heavy rainfall occurring in Australia during this time. For example, analysis of multi-day rainfall extremes during October 2010 to March 2012 showed limited evidence for a change in the probability of extreme SE Australian rainfall associated with La Niña events under late 20th century anthropogenic forcings using Coupled Model Intercomparison Project Phase 5 (CMIP5) models [*King et al.*, 2013] (hereafter referred to as K13). In addition, using an Attribution of Climate-related Events (ACE) approach, human influences from GHGs were found to have increased the probability of above average rainfall in eastern Australia in March 2012 by 5-15% [*Christidis et al.*, 2013b] (hereafter referred to as C13).

The K13 and C13 studies may appear to present contradictory results about the anthropogenic contribution to heavy rainfall in the eastern Australian region during 2011-2012, but rather they highlight the complexity of attempting to disentangle multiple climate influences on extreme rainfall. In particular, they suggest potential sensitivity of event attribution studies to the parameters selected in constructing an attribution framework. Event attribution provides a means of understanding recent observed events and useful information for adaptive decision making [*Stott et al.*, 2012]. Reliable attribution assessments are required, while ambiguous or confusing attribution statements do not help our understanding of changing probabilities of extreme events. Previous studies have also helped highlight the inherent complexity in understanding heavy rainfall events that warrants further investigation [*Shiogama et al.*, 2013; *Christidis et al.*, 2013b]. However, they have not addressed to what extent an attribution statement depends on the framework utilised. Is the attribution of Australia's extreme rainfall of 2010-2012 dependent on experimental design?

Here, we employ multiple detection and attribution model datasets, including fully coupled experiments and those driven by prescribed, observed sea surface temperatures, to investigate the possible anthropogenic and natural influences on Australian rainfall during 2010-2012. The aims of this study are to 1) examine the contributions of anthropogenic climate change and the La Niña contribution to the record seasonal rainfall occurring during 2010-2011 and to 2) assess to what extent this assessment depends on the model datasets utilised. A comprehensive attribution of the seasonal extreme rainfall occurring in Australia during 2010-2012 has not been undertaken and would prove useful for evaluating potential future changes in damaging climate events of this nature. Furthermore, the utility of extreme event attribution statements relies on establishing meaningful assessments of attributable changes in risk. Is reliable attribution possible for Australia's heavy 2010-2012 rainfall?

This paper is structured as follows: in Section 2, the climatological setting for Australia for 2010 to 2012 is described and in Section 3, we outline the models, experiments and attribution approach used. Section 4 evaluates the model statistics against observations and Section 5 assesses the anthropogenic influence on Australia's extreme rainfall. Section 6 discusses the influence of ENSO conditions on the extreme rainfall and finally conclusions are given in Section 7.

2. Observations

2.1 Climatological summary

Australia experienced its wettest two-year period on record during 2010-2012 [*Bureau of Meteorology*, 2012a]. On shorter timescales, record high daily accumulations were observed over large areas, with records broken at numerous stations [*Bureau of Meteorology*, 2012b]. The heavy rainfall occurring during 2010-2012 was particularly notable because of the spatial extent of precipitation anomalies. Average Australian conditions during 2010-2012 are summarised in Figure 1.

The 2010-2012 period was also characterised by extended La Niña conditions. The La Niña event beginning in late 2010 was particularly strong, and while La Niña conditions waned in the austral winter in 2011, a weaker, persistent La Niña re-emerged in the austral spring, and remained through the 2011-2012 summer months [*Bureau of Meteorology*, 2012a]. Typically, La Niña events are characterised by warm ocean waters and associated tropical convection in northern Australia and increased southeast Australian rainfall (Fig. 2). Furthermore, during this period, anomalously warm sea surface temperatures (SST) were observed to the north of Australia and in the eastern Indian Ocean. These likely enhanced Australian precipitation through enhanced inflow of low level water vapour and resulting increase in the total amount of precipitable water [*Evans and Boyer-Souchet*, 2012]. Observed SST anomalies in this region were up to 2°C warmer than those recorded during previous La Niña events.

2.2 Observational datasets

We utilise gridded observational datasets from various sources as a basis for comparison with model results. Observed monthly total rainfall amounts were calculated from the Australian Water Availability Project (AWAP) gridded dataset [*Jones et al.*, 2009]. We also use the median ensemble member of the HadCRUT4 gridded dataset of monthly surface air temperatures [*Morice et al.*, 2012] to assess observed ENSO variability and Australian rainfall anomalies associated with La Niña conditions. We then define three regions and area-average precipitation anomalies were calculated for eastern Australian (EA), southeastern Australian (SEA) and Australian (AUS) regions (Fig. 1).

3. Models

Model results were obtained from three distinct datasets (Table 1). First, we analysed precipitation simulated by 16 global climate models participating in CMIP5. Next, we utilised two sets of simulations conducted as part of the ACE initiative, in which ensembles of simulations are produced representing the recent climate with, and then without, the effects of human influences [*Stott et al.*, 2012]. These ACE experiment suites analysed here are based predominantly on the CAM5.1 [*Stone et al.*, in preparation] and HadGEM3-A [*Christidis et al.*, 2013a] models.

3.1 Model datasets

3.1.1 CMIP5

We investigate Australian precipitation using several standard CMIP5 experiments [*Taylor et al.*, 2012], summarised in Table 1. First, we analyse the historical experiment, simulating the climate of 1850 to 2005, using changing atmospheric compositions due to observed anthropogenic and volcanic influences, solar forcings and emissions of short-lived species from natural and anthropogenic aerosols. Additional CMIP5 simulations were also analysed, in order to separate anthropogenic and natural influences on 20th century climate. Specifically, we use the CMIP5 pre-industrial control (piControl) and historical natural-only (historicalNat) experiments. In the historicalNat detection and attribution experiment, each participating model is run over the period of 1850-2005, although no time evolving anthropogenic forcings are applied. In this study, the historicalNat and piControl experiments both provide the "world that might have been" counterpart to the anthropogenically-forced experiments, although the control experiment is only an approximation of the natural climate that provide many model years for analysis. We also utilise the standard RCP8.5 experiment (Representative Concentration Pathway with high emissions for the 21st century), to investigate changes during model years 2006-2020. We use this scenario as it is most representative of global CO_2 emissions that occurred from 2005 to present [*Peters et al.*, 2012] and hence most pertinent for investigating extreme rainfall occurring during 2010-2012 over Australia.

Results are presented from the CMIP5 historical experiment for the period of 1976-2005, encompassing the period of most substantial anthropogenic forcing and greatest likely distinction

from the piControl experiment. In addition to modelled precipitation, we assess Australian rainfall anomalies associated with La Niña conditions using simulated surface temperatures. We calculated the historical simulation NINO3.4 and precipitation anomalies from different climatologies. Historical SST anomalies for the NINO3.4 region are computed relative to a 30-year running mean, while precipitation anomalies are determined relative to the average in the first 50 years of the simulation (1850-1900). The rainfall anomalies were computed relative to the early period (1850-1900) so that the forced changes in rainfall could be assessed, while the trend in SSTs was removed using the running mean. The piControl anomalies were determined relative to the long-term mean, Data are presented from all available piControl years, as a basis for comparison with greenhouse gas-forced experiments. For the RCP8.5 experiment, temperature anomalies are calculated relative to the 2006-2020 period, while precipitation anomalies are calculated relative to an 1850-1900 climatology derived from the associated historical experiment, with model years 2006-2020 considered here.

3.1.2 CAM5.1

We also examine Australian rainfall changes in a set of parallel experiments conducted as part of the ACE initiative, with simulations run by the Lawrence Berkley National Laboratory [*Stone et al.*, in preparation]. Unlike the coupled CMIP5 experiments, these are atmosphere-only model simulations, driven by prescribed sea surface temperatures. Simulations were conducted using the CAM5.1 atmospheric model at both 1° and 2° horizontal resolutions, with 1°x1° resolution experiments utilised hereafter. For this contribution to the ACE project, 50 simulations were run with evolving observed ocean surface temperatures, sea ice coverage, greenhouse gas and tropospheric aerosol concentrations, stratospheric ozone, stratospheric volcanic aerosols and solar luminosity over the last 50 years (All-Hist). Each realisation had slightly different initial conditions.

Another set of 50 simulations (NonGHG-Hist) was then run with greenhouse gas concentrations maintained at pre-industrial levels, and with ocean surface temperatures cooled according to estimates of the warming pattern attributable to anthropogenic emissions. This cooling is estimated using the methodology of Pall et al. [2011a], utilising simulations of the HadCM3 model [*Stott et al.*, 2006] run with observed historical variations in various anthropogenic and natural

forcings. The warming attributable to GHGs is calculated using an optimal total least squares regression analysis [*Allen and Stott*, 2003; *Stott et al.*, 2003] based on both HadISST gridded observed temperatures [*Rayner et al.*, 2006] and HadCM3 simulations. The magnitude of the changes in SSTs attributable to each forcing is estimated by regressing the corresponding modelled SST patterns against the observed SST patterns and the total attributable ocean warming is then a linear combination of these patterns. The attributable warming (ΔSST) is subtracted from the SSTs and used as a boundary condition for the NonGHG-Hist ensemble members.

3.1.3 HadGEM3-A

We also analyse data based on the Hadley Centre Global Environmental Model version 3-A (HadGEM3-A). HadGEM3-A is the atmosphere-only component of HadGEM3 (Hewitt et al. 2011), run at a N96 horizontal resolution (1.25° longitude by 1.875° latitude) with 38 vertical levels. Comprehensive details of the model description and experimental design are provided by Christidis et al. [2013a]. These experiments are also atmosphere-only simulations, driven by prescribed sea surface temperatures. We primarily utilise the HadGEM3-A model dataset to assess the potential model-dependence of climate attribution statements. In particular, this dataset is useful as anthropogenic SST contributions are estimated from various, distinct coupled models, which are summarised in Table 2.

Two experiment sets were conducted using HadGEM3-A, simulating the climate with and without human influences. Each experiment consists of an ensemble of simulations with different climatic forcings, different SSTs and sea ice specifications. For the simulation of the actual climate (ALL), experiments are driven by anthropogenic forcing factors that comprise changes in well-mixed greenhouse gases, aerosols (sulfate, black carbon, and biomass burning), tropospheric and stratospheric ozone, and land-use changes, together with natural forcings from volcanic aerosols and solar irradiance. In contrast, the simulations of the climate without human influences include only natural volcanic and solar irradiance forcing factors. For these ‘natural’ world simulations (NAT), an estimate (ΔSST) of the anthropogenic change in the SSTs is subtracted from the HadISST [*Rayner et al.*, 2006] boundary data.

Ensembles were generated for each experiment by systematically sampling model uncertainty. First, a perturbed physics approach was used, where random perturbations are introduced to the model to represent the uncertainty in a number of parameters of atmospheric and surface physics, such as in large-scale clouds, convection, radiation, boundary layer and land surface processes. Second, a stochastic kinetic energy backscatter scheme was used to generate the model ensembles. In total, for the years 2010 and 2011, at least 99 ensemble members of the real world climate (ALL) were conducted using HadGEM3-A. Next, another set of 99 simulations (NAT) was then performed with greenhouse gas and aerosol concentrations maintained at pre-industrial levels, with estimates of anthropogenic SST warming determined each from the HadCM3, HadGEM1 and HaGEM2 models. This provides at least 297 realisations of the climate of the 'world that might have been' without human influences. For 2012, additional ensembles were completed. In total, 594 ensemble members of the real world climate exist using HadGEM3-A and estimates of anthropogenic SST warming were determined from a wider variety of models that also participate in CMIP5 (CSIRO-MK3-6L, CanESM2 and HadGEM2). As each simulated year (running September to August) was conducted separately, we consider only Australian precipitation in ONDJFM and DJF seasons with this dataset.

3.2 Data processing

Modelled and observed precipitation (pr) and near-surface air temperature (SAT) variables were processed into a common format. First, data were re-gridded onto a common 2.5° by 2.5° horizontal grid and average precipitation calculated each region. Precipitation anomalies in each of these regions were investigated as two year averages and also for April-March (ANN), summer (December to February, DJF) and the northern warm season (October to March, ONDJFM) periods. To account for inter-model differences in simulating Australian precipitation regimes, regional precipitation anomalies for CMIP5 models were calculated as standardised precipitation anomalies (as a percentage of normal rainfall, as defined by the climatological mean). This approach is used to remove the mean bias associated with each individual CMIP5 model and allows models and observation to be readily compared against each other for all seasons and regions. For the ACE model datasets, we consider area-average precipitation accumulations. In addition, as the rainfall

occurring in the heavily populated region of southeastern Australia was more extreme than over the larger regions, this study focuses primarily on the influences on SEA rainfall during 2010-2012.

3.3 Attribution of event risk

For each model dataset, the difference in probability of rainfall extremes in the natural and anthropogenically-forced simulations is assessed using Fraction of Attributable Risk (FAR). This is an expression of the fraction of risk of a particular threshold being exceeded (i.e. an event) that can be attributed to a particular influence. FAR was calculated as

$$FAR = 1 - \frac{P_{NAT}}{P_{ALL}},$$

where P_{NAT} denotes the probability of an event occurring in a reference state and P_{ALL} under a parallel forced state [*Stone and Allen*, 2005]. The FAR values were calculated by comparing the probability of unusual rainfall in the various model simulations, as determined by the number of times a threshold was exceeded, relative to the total sample size.

As only a single FAR is obtained from the model temperature distributions for each experiment, an assessment of uncertainty associated with FAR estimates was obtained by bootstrap resampling model FAR values 1000 times, using sub-samples of only 50% of available model simulations for each case. A distribution of possible FAR values was calculated. To indicate the spread of FAR values, we provide two estimates of the FAR value, which are exceeded by 50% (best estimate) and 90% (very likely) of the values in the bootstrapped FAR distributions. FAR values are reported as here as, FAR X/Y, where X is the best estimate value and Y the very likely value. We also calculated FAR values based on exceeding a series of thresholds defined by the observed precipitation mean ("average"), one standard deviation above normal ("heavy") and two standard deviations above normal ("extreme") [*Christidis et al.*, 2013b].

We also consider the change in the risk of a particular threshold being exceeded (i.e. an event) that can be attributed to simulated La Niña conditions. In this case, FAR was calculated as

$$FAR = 1 - \frac{P_{ElNino/Neutral}}{P_{LaNina}},$$

where $P_{ElNiño/Neutral}$ denotes the probability of an event occurring under neutral or positive NINO3.4 conditions and $P_{LaNiña}$ under negative NINO3.4 conditions. La Niña events were defined in the CMIP5 models when NINO3.4 negative SAT anomalies were larger than -0.5°C for at least six consecutive months during the year from April to March.

We employ similar methods for examining changes in the risk of extreme rainfall in each of the model datasets using fraction of attributable risk. However, it should be noted that the FAR values estimated with the coupled (CMIP5) and atmosphere-only (CAM5.1 and HadGEM3-A) models are not directly comparable. We first use the coupled models to investigate the changes in the odds of an extreme event in the general case, under any climatological conditions. The atmosphere-only models, however, are constrained by observed SSTs and hence retain information about modes of variability such as prevailing ENSO conditions. For example, the changes in odds of a heavy rainfall event occurring during a La Niña episode evaluated using the atmosphere-only models is estimated for this particular ENSO phase. Hence, the various sets of models provide complementary, rather than directly comparable, information about the changing likelihood of extremes due to anthropogenic forcings.

4. Evaluation of model statistics

Before an assessment of the relative influences of natural and human factors on the heavy Australian rainfall can be made, it is necessary to evaluate the performance of the models utilised. Christidis et al. [2013a] note that to meaningfully attribute changes in the odds of an extreme event to a particular cause, the model must capture the right mechanisms, with realistic frequency and characteristics, necessary to reproduce the event under consideration. Here, we investigate whether the models utilised realistically represent observed variability in both Australian heavy rainfall and ENSO conditions.

4.1 CMIP5

Models participating in CMIP5 were selected for inclusion based on several criteria, including 1) their representation of monthly surface air temperature variability in the NINO3.4 region, 2) their representation of Australian rainfall variability and 3) rainfall amount associated with ENSO conditions.

First, we compared observed and simulated SAT variability in the NINO3.4 region in the historical experiments for all CMIP5 participating models available for analysis on the Australian node of the Earth System Grid (ESG). Models were assessed against observed variability in the HadCRUT4 gridded dataset [*Morice et al.*, 2012] using a bootstrap resampling method, whereby we generated 10,000 timeseries of 80-year length, based on observed SAT anomalies. A spread of plausible NINO3.4 standard deviations was obtained from the bootstrap process and CMIP5 models were excluded from further analysis as physically unrealistic in instances where the simulated variability was outside of the bootstrapped 5^{th}-95^{th} percentile window derived from observations (Fig. 3a). Next, we compared the observed and simulated mean and standard deviation of seasonal precipitation amounts using a similar bootstrapping method and defined a physically realistic 5^{th}-95^{th} percentile window based on observed rainfall. This was repeated for each analysed region, for each temporal average considered. Finally, we assessed the La Niña–Australian rainfall relationship simulated by each CMIP5 model Simulated average Australian precipitation anomalies associated with La Niña conditions were compared to observed rainfall anomalies, using the described bootstrapping method (see Fig. 3b and 3c for example of DJF rainfall for southeastern Australia).

Models were included in this study in the case where they are realistic compared to observation for all three criteria (NINO3.4 variability, AUS rainfall variability, and La Niña-associated mean rainfall and rainfall variability). Ultimately, 16 models were available for analysis as adequately representing natural internal variability of Australian heavy rainfall and ENSO conditions (Table 2), providing a sufficiently large ensemble for investigating heavy seasonal rainfall in Australia.

4.2 CAM5.1

A similar approach was used to evaluate the statistics of Australian rainfall in the CAM5.1-based experiments. Unlike the CMIP5 fully coupled simulations, the CAM5.1 simulations are driven by prescribed, observed sea surface temperatures and hence the monthly NINO3.4 variability is not explicitly assessed here. Rather, we compare simulated precipitation mean and variability in each season and each region for extended All-Hist simulations extending from 1959 to 2012 and assess the validity of modelled precipitation amount and variability against observations. Overall, we find that the representation of rainfall is variable between regions, with model biases apparent in regions encompassing the wet tropics of northern Australia, particularly during the monsoon season. Simulated mean rainfall is most similar to observed for the southeastern Australian region. In some cases, the model underestimates rainfall variability, compared with the synthesised observed range, particularly for the east and southeastern Australian region in the warm seasons. In this case, attribution statements may be conservative, as the model simulations are potentially not capturing the full extent of observed extreme seasons.

Given the variable agreement between modelled and observed rainfall variability, we consider probabilistic changes in rainfall exceeding a range of thresholds, rather than a single thresholds used in other studies considering temperature extremes [*Stott et al.*, 2004; *Lewis and Karoly*, 2013]. Furthermore, due to the differences between observed and simulated Australian rainfall, we consider results from these SST-driven experiments as complementing the fully coupled model simulations and we focus on SEA, where mean rainfall is most similar to observed.

4.3 HadGEM3-A

The characteristics of Australian rainfall simulated using HadGEM3-A have been evaluated in the previous C13 attribution study and more extensively again in Christidis et al. [2013a]. In this study, model skill in simulating rainfall over northern and southern Australia was assessed using reliability diagrams and a comprehensive evaluation of model statistics was undertaken. The model performed well against observations in the southern region, but the model interannual variability was found to be higher than observed for northern Australia. Model skill was different for warm and wet, and cold and wet events, with the former best represented within the model, where events were

defined as the upper tercile of the 1971–2000 climatology calculated from NCEP–NCAR reanalysis. Overall, the model was found to adequately represent the statistics of high-precipitation events in most instances. Similarly, in the C13 study, simulated mean rainfall over eastern Australia occurring in March was assessed using reliability diagrams from a five-member ensemble of multi-decadal simulations of actual climate. In this case, the model was found to be a reliable tool for examining regional rainfall influences as the model forecast probability was consistent with the frequency of heavy rain in observations of eastern Australia.

As the HadGEM3-A-based detection and attribution model datasets has previously been evaluated extensively [*Christidis et al.*, 2013a], we do not explicitly evaluate the model in our study. Given the previously established limitation in representing heavy rainfall events in northern Australia, our analysis using the HadGEM3-A model focuses on the southeastern Australian region. In addition, the focus of analysis using this model dataset is on the potential sensitivity of event attribution attempts to model-dependent anthropogenic sea surface temperature estimates [*Christidis et al.*, 2013b], which cannot be evaluated against observations.

5. Anthropogenic influences on Australian rainfall

5.1 CMIP5

There is little difference between the probability distributions (PDFs) of rainfall in the CMIP5 piControl and historical simulations, and the historicalNat and historical simulations, as estimated using a kernel smoothing function. A Kolmogrov-Smirnov test indicates that the respective piControl and historical PDFs are not significantly different (at the 5% level) from each other for most regions, for most temporal averages considered. Next, we compared the probability density functions of heavy rainfall associated with simulated La Niña events for the piControl and historical experiments for Australia, eastern Australia and southeastern Australia for the annual, DJF and ONDJFM seasons. We then considered the likelihood of exceeding a series of seasonal rainfall thresholds, whereby seasonal average rainfall anomalies exceeded one standard deviation above the standardised precipitation mean (“heavy”) and two standard deviations above normal (“extreme”) determined from the AWAP observational record. The probabilities of rainfall associated with above average

rainfall during simulated La Niña events in the piControl and historical experiments are shown in Figure 4.

We examined the difference in risk of unusual rainfall between the historical experiment (years 1976-2005) and piControl experiment (all years) by comparing the number of times each threshold is exceeded, relative to the total simulated sample size. The calculated FAR values are highly sensitive to the selection of rainfall thresholds, region and season considered and the calculated FAR distributions, determined by bootstrap resampling, also demonstrate large spreads of values. The probability of heavy rainfall was also considered in the RCP8.5 experiments for models years 2006-2020, where the FAR was again found to be sensitive to the threshold used and the region and season considered. This highlights that attempts at attribution using the CMIP5 dataset may be sensitive to the experiment design and parameters utilised in an attribution framework. Attribution statements for above average, heavy or extreme rainfall are unlikely to be robust based on rainfall probabilities calculated from the CMIP5 historical, RPC8.5 and piControl experiments.

5.2 CAM5.1

We also examined the likelihood of heavy Australian rainfall using atmospheric models driven by prescribed sea surface temperatures, which provides specific information about the changing odds of extreme rainfall under particular ENSO conditions. In this case where simulations are forced by observed SSTs, rainfall occurrence in the 'real world' experiment (All-Hist) is compared directly to the 'world that might have been' (NonGHG-Hist) experiment with no anthropogenic influences. The contribution of anthropogenic sea surface changes to extreme Australian rainfall can then be made explicitly, with comparisons made between these experiments for 2010, 2011 and the two-year average for 2010 through to 2012. As the CAM5.1 model is best able to represent observed rainfall for the southeastern Australian region, differences between experiments are explored here.

Simulated rainfall accumulations are generally lower for 2011-2012 than for the previous year, and the distinction between the All-Hist and NonGHG-Hist rainfall distributions is clearer for 2011-2012 (Fig. 5). Increases in the probability of extreme rainfall associated with anthropogenic

forcings in the All-Hist experiment are simulated for all seasons for southeastern Australia for 2011-2012. The calculated FAR values demonstrate some increase in the risk of extreme 2011-2012 rainfall in southeastern Australia that can be attributed to greenhouse gases (April-March FAR 0.30/-0.30; ONDJFM FAR 0.50/-0.10; DJF FAR 0.40/0.10). However, the large uncertainties relating to the FAR values (calculated through bootstrap resampling) indicate that these values are not likely to be robust to changes in the attribution framework. For the comparatively stronger La Niña event of 2010-2011, the attributable risk of above average, heavy and extreme rainfall due to anthropogenic influences is again sensitive to the rainfall threshold and seasons selected. Overall, the largest increase in risk attributable to anthropogenic causes occurs for extreme rainfall occurring over April to March (FAR 0.38/-0.20) with the lowest FAR value for DJF (-0.10/-0.44). The anthropogenic influence on the record rainfall was no clearer when changes occurring over a 2-year period in the CAM5.1 dataset were considered. Combining rainfall for the two years in the CAM5.1 simulations, the calculated April-March southeastern Australian FAR values for above average (FAR 0.12/-0.30), heavy (FAR 0.18/-0.17) and extreme (FAR 0.53/0.10) rainfall were similar to that for 2011-2012 alone.

The ambiguous influence of anthropogenic forcings on the impact of extended (two-year) La Niña events on Australian rainfall is supported with the parallel historical and piControl CMIP5 coupled model experiments. Observed La Niña events are generally briefer than El Niño events and extended La Niña events are rare, so we synthesised a set of extended (or double) La Niña events by resampling designated model La Niña years into two-year blocks using a bootstrapping approach. This approach is first evaluated by resampling gridded observational Australian rainfall (AWAP) data associated with La Niña conditions (determined from the HadCRUT4 dataset), indicating that Australian region rainfall changes associated with synthesised, extended La Niña events were similar to those occurring during the 2010-2012 period. This resampling approach was applied to modelled La Niña years in the piControl and historical simulations to synthesise extended, simulated La Niña conditions. The resulting FAR values were again found to be sensitive to the regions and seasons analysed and thresholds used and do not permit any clear attribution statement being made for the longer time period considered.

5.3 HadGEM3-A

Unusual southeastern Australian rainfall was next investigated with the HadGEM3-A dataset, using estimates of the anthropogenic contribution to SSTs calculated from three distinct models and subsequently removed to provide a range of approximations of the natural climate. As distinct models were used for estimating the anthropogenic SST and sea ice patterns for 2010-2011 and 2011-2012, we consider only the DJF and ONDJFM seasonal average precipitation changes between the ALL and NAT experiments (Fig. 6 and 7). In addition to the sensitivity of anthropogenic changes in Australian rainfall to the region and season analysed, there are clear differences in the probability of above average, heavy and extreme rainfall associated with the particular model used for the ΔSST estimate. For example, there are distinct differences in the tails of the probability distributions determined using the HadGEM1 model and the HadGEM2 and HadCM3 models, particularly for December 2010 to February 2011 (Fig. 6d-f).

The largest inter-model differences occur during the comparatively weaker La Niña event for the 2011-2012 seasonal southeastern Australian rainfall averages. For this region, disparate rainfall responses are simulated using the CSIRO-Mk-3.6L model, compared with the other models used to estimate the anthropogenic ΔSST patterns. Also, distinct FAR values are computed using each model estimate. Similar anthropogenically-driven increases in risk associated with extreme southeastern Australian rainfall are calculated during summer and the northern warm season for 2011-2012 using the HadGEM2 (ONDJFM FAR 0.72/0.58; DJF FAR 0.66/0.44) and CanESM2 (ONDJFM FAR 0.63/0.46; DJF FAR 0.69/0.48) model estimates of anthropogenic SST warming. However, an anthropogenic-related decrease in risk of extreme rainfall is calculated using the CSIRO-Mk-3.6L to estimate anthropogenic SST warming (ONDJFM FAR -0.14/-0.29; DJF FAR -0.19/-0.47). Using these three separate models to first estimate anthropogenic SST influences, it is clear that attempts to attribute unusual rainfall to anthropogenic forcings in this case is model-dependent.

6. ENSO-influences on heavy Australian rainfall

The unusual Australian rainfall is also considered in relation to the strong, persistent La Niña events that characterised 2010-2012, as such conditions are typically related to enhanced tropical

convection in northern Australia and increased southeastern Australian rainfall (Fig. 2). Can the record rainfall be attributed to natural climate variability resulting from the observed, strong La Niña conditions? We investigated changes in the probability of rainfall in CMIP5 historical simulations associated with La Niña and El Niño/neutral conditions (Fig. 8) to assess the role of NINO3.4 on regional rainfall extremes. Model years that did not exhibit La Niña conditions were otherwise categorised as El Niño/neutral years.

There is a clear shift in the distribution of southeastern Australian rainfall towards wetter conditions during La Niña events, compared with El Niño/neutral conditions, for all seasonal averages considered. Furthermore, there is a large increase in the probability of heavy and extreme rainfall that can be attributed to La Niña conditions, including a very likely (90%) greater than five-fold increase in the risk of heavy or extreme rainfall during April-March in this region attributable to La Niña SST anomalies (FAR 0.83). While there is little attributable change in above average rainfall due to varying ENSO conditions, the increase in risk of heavy or extreme rainfall due to La Niña variability is robust across the analysed regions and seasons. We then compared rainfall occurring in two All-Hist years simulated using the CAM5.1 model with all forcings (Fig. 9), showing that simulated heavy SEA rainfall during the strong La Niña conditions of 2010-2011 is more likely than during the weak El Niño of 2009-2010. The increase in the probability of heavy and extreme SEA rainfall relates to SST difference between 2009-2010 and 2010-2011. These differences include changes associated with the varying ENSO phases and provide broad support for the La Niña-driven increase in risk of extreme Australian rainfall determined from the fully coupled CMIP5 models. Although these two years are clearly not representative of all observed La Niña and El Niño conditions, the increase in likelihood of heavy and extreme SEA rainfall in the 2010-2011 simulations reflects the increase in probability of unusual SEA rainfall also calculated from the CMIP5 coupled models during La Niña phases.

We have demonstrated that the probability of unusual seasonal Australian rainfall like that occurring during 2010-2012 is influenced by La Niña conditions. Do changing boundary conditions from the anthropogenic-warming trend also influence the relationship between Australian rainfall and ENSO? We compared NINO3.4 and precipitation anomalies between anthropogenically-driven and

natural-only CMIP5 experiments, using the suite of piControl and historical simulations (Fig. 10). The relationship between temperature variability in the NINO3.4 region and rainfall variability in southeastern Australia, as well as the AUS and EA regions, is found to be relatively insensitive to experimental forcings. That is, in each region and season, similar rainfall responses, associated with NINO3.4 conditions, are recorded for the control and anthropogenically-forced experiments.

7. Discussion and conclusions

We estimated anthropogenic and natural influences on the unusual Australian rainfall of 2010-2012 using three model datasets, including a suite of fully coupled models (CMIP5) and two atmosphere-only model datasets (CAM5.1 and HadGEM3-A) forced by observed SSTs. For each dataset, two parallel experiments were conducted, one including and one excluding anthropogenic influences from long-lived greenhouse gases. Changes in the probability of average, heavy and extreme Australian, eastern and southeastern Australian rainfall associated with anthropogenic forcings were then calculated for each model dataset. What influenced Australia's rainfall over 2010-2012? The attribution of unusual rainfall like that occurring in Australia during this period to anthropogenic forcings was equivocal. Using the atmosphere-only models, simulated increases in the probability of extreme rainfall associated with greenhouse gases was clearer for seasonal averages over 2011-2012, than during 2010-2011 when comparatively stronger La Niña conditions prevailed. The anthropogenic influence on the likelihood of extreme rainfall was somewhat clearer using experiments driven by observed sea surface temperatures (CAM5.1 and HadGEM3-A) than in the fully coupled CMIP5 models. However, the calculated fraction of attributable risk values were also found to be sensitive to the region, season and threshold utilised.

Previous attempts to attribute heavy Australian rainfall occurring during this record period to anthropogenic influences have also produced uncertain attribution statements. In the first such study investigating March 2012 eastern Australian rainfall using ACE SST-forced simulations, C13 found that anthropogenic influences on the climate increases the chances of above average rainfall by 5-15%, although the impact on extreme precipitation was more uncertain. Similarly, K13 found limited evidence for a robust change in the risk of heavy SEA 5-day rainfall during this time that can be

attributed to long-term human influences through CMIP5 historical runs. Generally, the small but highly sensitive shift in heavy rainfall probabilities determined in these previous studies is expected from general thermodynamic arguments of heavy precipitation increasing with increasing atmospheric water vapour due to anthropogenic warming trends [*Pall et al.*, 2007; 2011b]. Nonetheless, recent studies have also emphasised the importance of dynamical component (i.e. changes in circulation), in addition to thermodynamic components, for changes in extreme precipitation with increasing greenhouse gas forcings [*Sugiyama et al.*, 2010]. As such, while thermodynamics are useful for providing general information, understanding specific precipitation changes requires consideration of both thermodynamics and dynamic components.

Our present study highlights the general difficulties in understanding the causes of observed heavy rainfall and disentangling multiple influences when attempting to attribute a specific precipitation event to a particular cause. The sensitivity of the attribution of heavy rainfall to the selected parameters such as thresholds, regions and seasons considered does not suggest that the attribution methods utilised are not appropriate for understanding rainfall extremes but rather that the change in risk of precipitation extremes is difficult to determine robustly given the degree of anthropogenic forcing, relative to the natural variability. The lack of statistically significant trends in observed Australian rainfall explains to some extent why the FAR values cannot be calculated precisely. Previous studies suggest that while determining the precise magnitude of anthropogenic contributions to extreme rainfall is currently uncertain [*Pall et al.*, 2011b; *King et al.*, 2013; *Christidis et al.*, 2013b],, robust attribution may be possible when considering changes in the probability of occurrence of large seasonal precipitation amounts in response to an intensified anthropogenic forcing over the next century [*Palmer and Raisanen*, 2002]. When considering temperature extremes, the estimated of FAR is likely to be more robust due to the stronger anthropogenic signal and clearer separation of natural-only and anthropogenically influenced distributions. For example, recent seasonal-scale temperature attribution studies have provided comparatively more robust attribution statements regarding anthropogenic influences on observed temperature extremes [*Stott et al.*, 2004; *Lewis and Karoly*, 2013].

We used various complementary model datasets to investigate influences on the observed Australian extreme rainfall. The FAR values estimated with coupled models are, however, not directly comparable to those estimated with the SST-driven atmosphere-only models, with each approach addressing slightly different research questions. In particular, the coupled models provide general information about the changes in the odds of extreme rainfall, whereas the atmosphere-only models provide specific information constrained by observed SSTs and hence retain certain modes of variability, such as ENSO. Theses approaches provide somewhat different information for understanding extremes. Attribution of heavy Australian rainfall with the coupled CMIP5 models was highly uncertain, while attribution was clearer using the atmosphere-only models, as the use of imposed boundary conditions reduces variability and a comparatively more robust estimate of the change in the odds of extreme precipitation could be determined.

In our present study, we find that the attribution of unusual rainfall to anthropogenic influences depends both on the models used and also on estimates of the anthropogenic SST warming component used to determine the counterfactual, natural-only conditions. Within the HadGEM3-A dataset, substantially different risk attribution statements were derived when anthropogenic SST estimates were made with the CSIRO-MK3-6L model than with either the CanESM2 or HadGEM2 models. This may result from warm SST biases, relative to observed, around northern Australia in the CSIRO-MK3-6L model [*Gordon et al.*, 2002]. Previous event attribution attempts have also reported that assessments were sensitive to model bias corrections [*Shiogama et al.*, 2013] and to the models used for estimates of anthropogenic SST contributions [*Pall et al.*, 2011b; *Christidis et al.*, 2013b]. The counterfactual, natural-only world used in event attribution studies clearly cannot be readily evaluated in a rigorous manner against observations of the real world, which is influenced by both natural and anthropogenic forcings. The boundary conditions used in establishing a 'natural' only set of simulations may be a major source of uncertainty in in attribution studies [*Christidis and Stott*, 2014]. As such, in complex precipitation-based event attribution studies, it may be useful to consider outputs from several model datasets and also various estimates of counterfactual conditions. In this case, an assessment of the sensitivity of any resulting attribution statement to the experimental design can be rigorously made.

As the heavy 2010-2012 Australian rainfall occurred during consecutive, strong La Niña events, we also investigated the possible contributions of the El Nino-Southern Oscillation to the observed rainfall. We use FAR to investigate changes in unusual rainfall associated with La Niña conditions as a novel approach to understanding the influence of modes of natural climatic variability on heavy seasonal rainfall, rather than relying purely only on statistical relationships between Australian rainfall and NINO3.4 anomalies [*McBride and Nicholls*, 1983]. The attribution of heavy and extreme Australian rainfall (like that occurring during 2010-2012) to the prevailing La Niña conditions was robust using the fully coupled CMIP5 historical simulations. There was a very likely (90%) five-fold increase in the risk of April-March extreme rainfall in SEA that could be attributed to simulated La Niña conditions. The influence of La Niña conditions on rainfall was discernible in each analysed region. Although there was a substantial La Niña influence on the likelihood of above normal Australian rainfall during this time, the extreme magnitude of the event also likely required unforced internal climatic variability [*Christidis et al.*, 2013b]. Overall, attribution to the prevailing La Niña conditions, compared to anthropogenic influences, demonstrates that FAR values are more robust where there is a clear separation of the differing rainfall distributions considered.

Acknowledgements

This research was supported by funding from the Australian Research Council Centre of Excellence for Climate System Science (grant CE 110001028). This work was also supported by the NCI National Facility at the ANU. We also thank the Dáithí Stone at the Lawrence Berkeley National Laboratory and Nikos Christidis and Peter Stott at the Met Office Hadley Centre for generously providing access to data. We acknowledge the World Climate Research Programme's Working Group on Coupled Modelling, which is responsible for CMIP, and we thank climate modelling groups for producing and making available their model output. For CMIP, the U.S. Department of Energy's Program for Climate Model Diagnosis and Intercomparison provides coordinating support and led development of software infrastructure in partnership with the Global Organization for Earth System Science Portals. Finally, we thank the two reviewers for their useful comments on the manuscript.

Figure Captions

Figure 1.

Observed precipitation anomalies (mm) for April 2010 to March 2012, relative to 1961-1990, from AWAP gridded data (A). Eastern Australian (EA), southeastern Australian (SEA) and Australian (AUS) regions are shown. Observed southeastern Australian rainfall anomalies (mm, relative to 1961-1990) for April-March (B), ONDJFM (C) and DJF (D). Average anomalies during 2010-2011 and 2011-2012 are shown by red squares. Linear trends were calculated for each season using a standard linear regression but were not found to be significant at the 10% level using a student's t-test.

Figure 2.

Scatter plots of observed Tmean anomalies (K) in the NINO3.4 region against area-averaged southeastern Australian precipitation anomalies (mm, relative to 1961-1990) for 1912-2011 for April-March (A), ONDJFM (B) and DJF (C). Average anomalies during 2010-2011 are shown by red squares. Lines of best fit for warm and cool NINO3.4 anomalies are calculated using ordinary least squares regression.

Figure 3.

(A) Comparison of observed and simulated NINO3.4 monthly surface air temperature variability (K) for observations and all CMIP5 models with historical experiments archived on the Australian ESG node. (B) As for panel A but showing southeastern Australian standardised DJF mean precipitation as a percentage of normal rainfall defined by the climatological mean) and (C) southeastern Australian standardised DJF precipitation variability (σ). In all plots, the mean observational value is shown by a cross and the 5^{th}-95^{th} percentile range indicated by horizontal dashed lines, as determined by bootstrap resampling observed values. Individual model realisations are shown by black squares and each model mean by red circles. Only models lying within the synthesised observed range for the three performance criteria are included in this study.

Figure 4

PDFs for CMIP5 historical (red, 1976-2005 only) and piControl (dark blue, all years shown relative to long-term mean) simulations for Australia (A-C), eastern Australia (D-F) and southeastern Australia (G-H) regions for April-March, ONDFM and DJF seasonal average standardised precipitation (as a percentage of normal rainfall as defined by the climatological mean) for above average rainfall in simulated La Niña years (NINO3.4 SAT anomalies were less than 0.5°C for at least six consecutive months during the year from April to March). Vertical dashed lines show thresholds for one ("heavy") and two standard ("extreme") deviations above climatological mean determined from AWAP observational data for years 1910-2012. The thresholds are based on observed rainfall under all ENSO conditions, so they appear in the dry tail of the distribution of above average simulated rainfall associated with La Niña years.

Figure 5

PDFs for CAM5.1 All-Hist (red) and NonGHG-Hist (dark blue) simulations for southeastern Australian April-March, ONDFM and DJF seasonal rainfall accumulations (mm) for 2010-2011 (left) and 2011-2012 (right). Vertical dashed lines show thresholds for mean accumulated precipitation (mm) ("average"), one ("heavy") and two standard ("extreme") deviations above climatological mean determined from AWAP observational data for years 1910-2012. As thresholds are determined using rainfall in all observed years, they appear in the dry tail of the rainfall distributions associated with the La Niña years of 2010-2012.

Figure 6

PDFs for HadGEM3-A ALL (red) and NAT (dark blue) simulations southeastern Australia region for ONDFM (left) and DJF (right) seasonal rainfall accumulations (mm) for 2010-2011. Vertical dashed lines show thresholds for mean accumulated precipitation (mm) ("average"), one ("heavy") and two standard ("extreme") deviations above climatological mean determined from AWAP observational data for years 1910-2012. As thresholds are determined using rainfall in all observed years, they appear in the dry tail of the rainfall distributions associated with the La Niña years of 2010-2012.

Figure 7

As for Figure 6 but showing 2011-2012 ONDJFM (left) and DJF (right) seasonal rainfall accumulations (mm).

Figure 8

PDFs comparing southeastern Australian standardised rainfall during La Niña (dark blue) conditions derived from CMIP5 historical simulations, with El Niño/neutral (red) conditions. Probability densities are shown for April to March (A), ONDFM (B) and DJF (C) rainfall anomalies. La Niña years are defined where simulated NINO3.4 SAT anomalies were less than 0.5°C for at least six consecutive months during the year from April to March. Vertical dashed lines show thresholds for mean standardised precipitation ("average"), one ("heavy") and two standard ("extreme") deviations above climatological mean determined from AWAP observational data for years 1910-2012.

Figure 9.

PDFs for CAM5.1 All-Hist simulations comparing southeastern Australian rainfall accumulations (mm) for 2010-2011 (dark blue) and 2009-2010 (red) conditions. Probability densities are shown for April to March (A), ONDFM (B) and DJF (C). Vertical dashed lines show thresholds for mean accumulated precipitation (mm) ("average"), one ("heavy") and two standard ("extreme") deviations above climatological mean determined from AWAP observational data for years 1910-2012.

Figure 10

Scatter plots of NINO3.4 surface air temperature anomalies (K) against area-average southeastern Australian standardised precipitation anomalies for (A) April to March, (B) ONDJFM and (C) DJF for historical (red) and piControl (blue) model years. Lines of best fit are also shown, calculated using ordinary least squares regression.

Table Captions

Table 1.

Summary of model datasets (CMIP5, CAM5.1 and HadGEM3-A) analysed, including the model experiments and forcings, number of simulations, type of ensemble, the model years analysed in this study and the baseline climatology used to calculate temperature anomalies.

Table 2

Summary of CMIP5-participating models used in this study, based on their representation of monthly surface air temperature variability in the NINO3.4 region, their representation of Australian rainfall variability and also rainfall associated with ENSO conditions. Details of models used in HadGEM3-A-based dataset analysed in this study are also shown.

References

Allen, M. R., and P. A. Stott (2003), Estimating signal amplitudes in optimal fingerprinting, part I: theory, *Climate Dynamics*, *21*(5-6), 477–491, doi:10.1007/s00382-003-0313-9.

Bureau of Meteorology (2012a), *Australia's wettest two-year period on record; 2010–2011. Special Climate Statement 38*.

Bureau of Meteorology (2012b), *Exceptional heavy rainfall across southeast Australia. Special Climate Statement 39*.

Christidis, N., and P. A. Stott (2014), Change in the Odds of Warm Years and Seasons Due to Anthropogenic Influence on the Climate, *Journal of Climate*, *27*(7), 2607–2621, doi:10.1175/JCLI-D-13-00563.1.

Christidis, N., P. A. Stott, A. A. Scaife, A. Arribas, G. S. Jones, D. Copsey, J. R. Knight, and W. J. Tennant (2013a), A New HadGEM3-A-Based System for Attribution of Weather- and Climate-Related Extreme Events, *Journal of Climate*, *26*(9), 2756–2783, doi:10.1175/JCLI-D-12-00169.1.

Christidis, N., P. A. Stott, D. J. Karoly, and A. Ciavarella (2013b), An Attribution Study of the Heavy Rainfall over Eastern Australia in March 2012, edited by T. C. Peterson, M. P. Hoerling, P. A. Stott, and S. C. Herring, *Bulletin of the American Meteorological Society*, *94*(9), S58–S61.

Evans, J. P., and I. Boyer-Souchet (2012), Local sea surface temperatures add to extreme precipitation in northeast Australia during La Niña, *Geophysical Research Letters*, *39*(10), doi:10.1029/2012GL052014.

Ganter, C., and S. Tobin (2013), Australia, in *State of the Climate in 2012*, vol. 94, edited by J. Blunden and D. S. Arndt, pp. S196–S198, *Bulletin of the American Meteorological Society*.

Gordon, H. B. et al. (2002), *The CSIRO Mk3 Climate System Model*, CSIRO Atmospheric Research Technical Paper 60.

Jones, D. A., W. Wang, and R. Fawcett (2009), High-quality spatial climate data-sets for Australia, *Australian Meteorological and Oceanographic Journal*, *58*(4), 233.

King, A. D., S. C. Lewis, S. E. Perkins, L. V. Alexander, M. G. Donat, D. J. Karoly, and M. T. Black (2013), Limited Evidence of Anthropogenic Influence on the 2011–12 Extreme Rainfall Over Southeast Australia, edited by T. C. Peterson, M. P. Hoerling, P. A. Stott, and S. C. Herring, *Bulletin of the American Meteorological Society*, *94*(9), S55–S58.

Lewis, S. C., and D. J. Karoly (2013), Anthropogenic contributions to Australia's record summer temperatures of 2013, *Geophysical Research Letters*, doi:10.1002/grl.50673.

Li, J. et al. (2013), El Niño modulations over the past seven centuries, *Nature Climate Change*, *3*(9), 822–826, doi:10.1038/nclimate1936.

McBride, J. L., and N. Nicholls (1983), AMS Journals Online - Seasonal Relationships between Australian Rainfall and the Southern Oscillation, *Mon. Wea. Rev.*

Morice, C. P., J. J. Kennedy, N. A. Rayner, and P. D. Jones (2012), Quantifying uncertainties in global and regional temperature change using an ensemble of observational estimates: The HadCRUT4 data set, *Journal of Geophysical Research Atmospheres*, *117*(D8), D08101, doi:10.1029/2011JD017187.

Nicholls, N. (2011), What caused the eastern Australia heavy rains and floods of 2010/11? *Bulletin of the Australian Meteorological and Oceanographic Society*, 33–34.

Nicholls, N., B. Lavery, C. Frederiksen, W. Drosdowsky, and S. Torok (1996), Recent apparent changes in relationships between the El Niño - Southern oscillation and Australian rainfall and temperature, *Geophysical Research Letters*, *23*(23), 3357–3360.

Pall, P., M. R. Allen, and D. A. Stone (2007), Testing the Clausius–Clapeyron constraint on changes in extreme precipitation under CO2 warming, *Climate Dynamics*.

Pall, P., T. Aina, D. A. Stone, P. A. Stott, T. Nozawa, A. G. J. Hilberts, D. Lohmann, and M. R. Allen (2011a), Anthropogenic greenhouse gas contribution to flood risk in England and Wales in autumn 2000, *Nature*, *470*(7334), 382–385, doi:10.1038/nature09762.

Pall, P., T. Aina, D. A. Stone, P. A. Stott, T. Nozawa, A. G. J. Hilberts, D. Lohmann, and M. R. Allen (2011b), Anthropogenic greenhouse gas contribution to flood risk in England and Wales in autumn 2000, *Nature*, *470*(7334), 382–385, doi:10.1038/nature09762.

Palmer, T., and J. Raisanen (2002), Quantifying the risk of extreme seasonal precipitation events in a changing climate, *Nature*, *415*(6871), 512–514.

Peters, G. P., R. M. Andrew, T. Boden, J. G. Canadell, P. Ciais, C. Le Quéré, G. Marland, M. R. Raupach, and C. Wilson (2012), The challenge to keep global warming below 2 °C, *Nature*, *3*(1), 4–6, doi:10.1038/nclimate1783.

Rayner, N. A., P. Brohan, D. E. Parker, C. K. Folland, J. J. Kennedy, M. Vanicek, T. J. Ansell, and S. F. B. Tett (2006), Improved Analyses of Changes and Uncertainties in Sea Surface Temperature Measured In Situ since the Mid-Nineteenth Century: The HadSST2 Dataset, *http://dx.doi.org/10.1175/JCLI3637.1*.

Shiogama, H., M. Watanabe, Y. Imada, M. Mori, M. Ishii, and M. Kimoto (2013), An event attribution of the 2010 drought in the South Amazon region using the MIROC5 model, *Atmospheric Science Letters*, doi:10.1002/asl2.435.

Stone, D. A., and M. R. Allen (2005), The End-to-End Attribution Problem: From Emissions to Impacts, *Climatic Change*, *71*(3), 303–318, doi:10.1007/s10584-005-6778-2.

Stott, P. A., D. A. Stone, and M. R. Allen (2004), Human contribution to the European heatwave of 2003, *Nature*, *432*(7017), 610–614, doi:10.1038/nature03089.

Stott, P. A., J. F. B. Mitchell, M. R. Allen, T. L. Delworth, J. M. Gregory, G. A. Meehl, and B. D. Santer (2006), Observational Constraints on Past Attributable Warming and Predictions of Future Global Warming, *Journal of Climate*, *19*(13), 3055–3069, doi:10.1175/JCLI3802.1.

Stott, P. A., M. Allen, N. Christidis, R. Dole, M. Hoerling, C. Huntingford, P. Pall, J. Perlwitz, and D. Stone (2012), Attribution of weather and climate-related extreme events, *WCRP Position Paper on ACE*. Available from: http://library.wmo.int/pmb_ged/wcrp_2011-stott.pdf (Accessed 16 March 2012)

Stott, P. A., M. R. Allen, and G. S. Jones (2003), Estimating signal amplitudes in optimal fingerprinting. Part II: application to general circulation models, *Climate Dynamics*, *21*(5-6), 493–500, doi:10.1007/s00382-003-0314-8.

Sugiyama, M., H. Shiogama, and S. Emori (2010), Precipitation extreme changes exceeding moisture content increases in MIROC and IPCC climate models, *Proceedings of the National Academy of*

Sciences, *107*(2), 571–575, doi:10.1073/pnas.0903186107.

Taylor, K. E., R. J. Stouffer, and G. A. Meehl (2012), An overview of CMIP5 and the experiment design, *Bulletin of the American Meteorological Society*, *93*(4), 485, doi:10.1175/BAMS-D-11-00094.1.

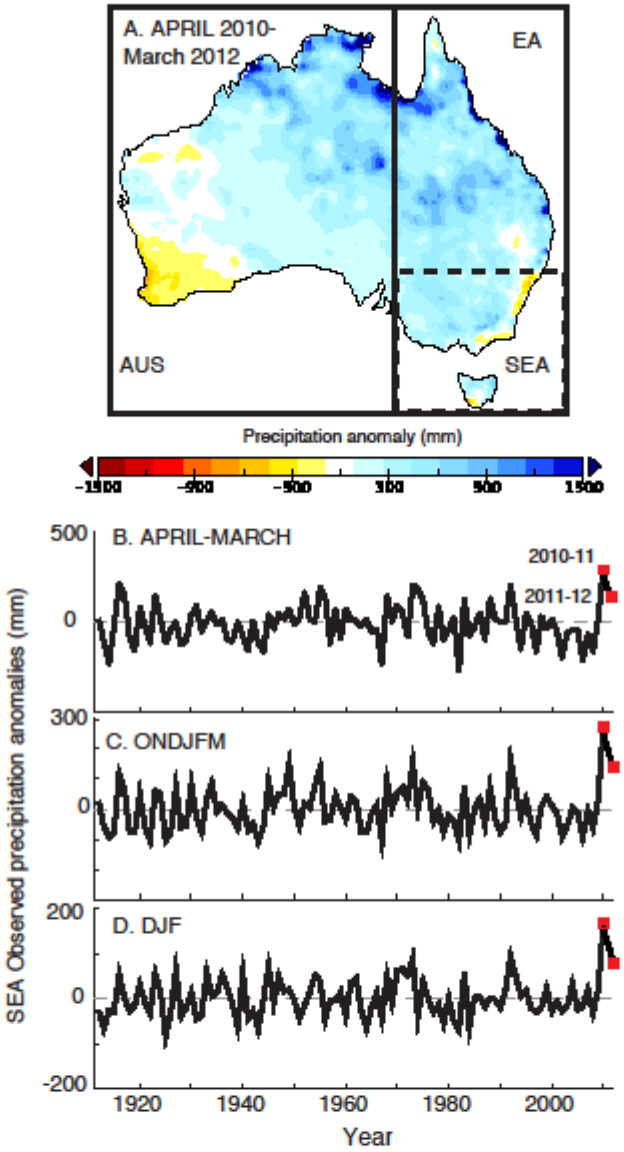

Figure 1.
Observed precipitation anomalies (mm) for April 2010 to March 2012, relative to 1961-1990, from AWAP gridded data (A). Eastern Australian (EA), southeastern Australian (SEA) and Australian (AUS) regions are shown. Observed southeastern Australian rainfall anomalies (mm, relative to 1961-1990) for April-March (B), ONDJFM (C) and DJF (D). Average anomalies during 2010-2011 and 2011-2012 are shown by red squares. Linear trends were calculated for each season using a standard linear regression but were not found to be significant at the 10% level using a student's t-test.

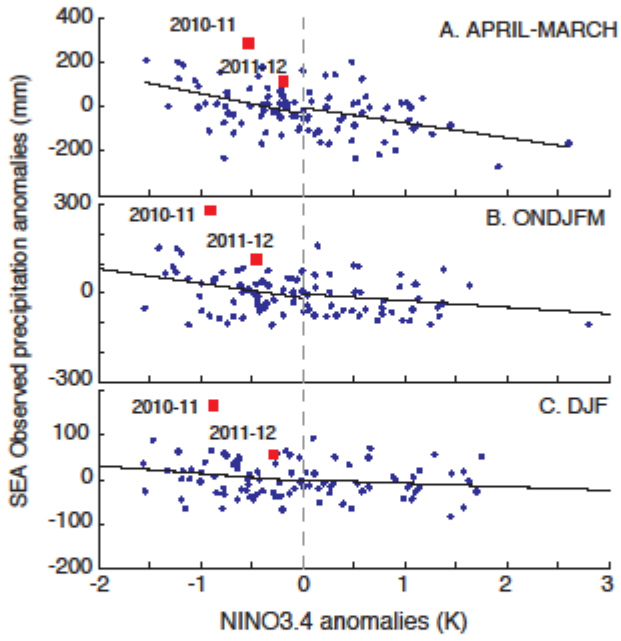

Figure 2.
Scatter plots of observed Tmean anomalies (K) in the NINO3.4 region against area-averaged southeastern Australian precipitation anomalies (mm, relative to 1961-1990) for 1912-2011 for April-March (A), ONDJFM (B) and DJF (C). Average anomalies during 2010-2011 are shown by red squares. Lines of best fit for warm and cool NINO3.4 anomalies are calculated using ordinary least squares regression.

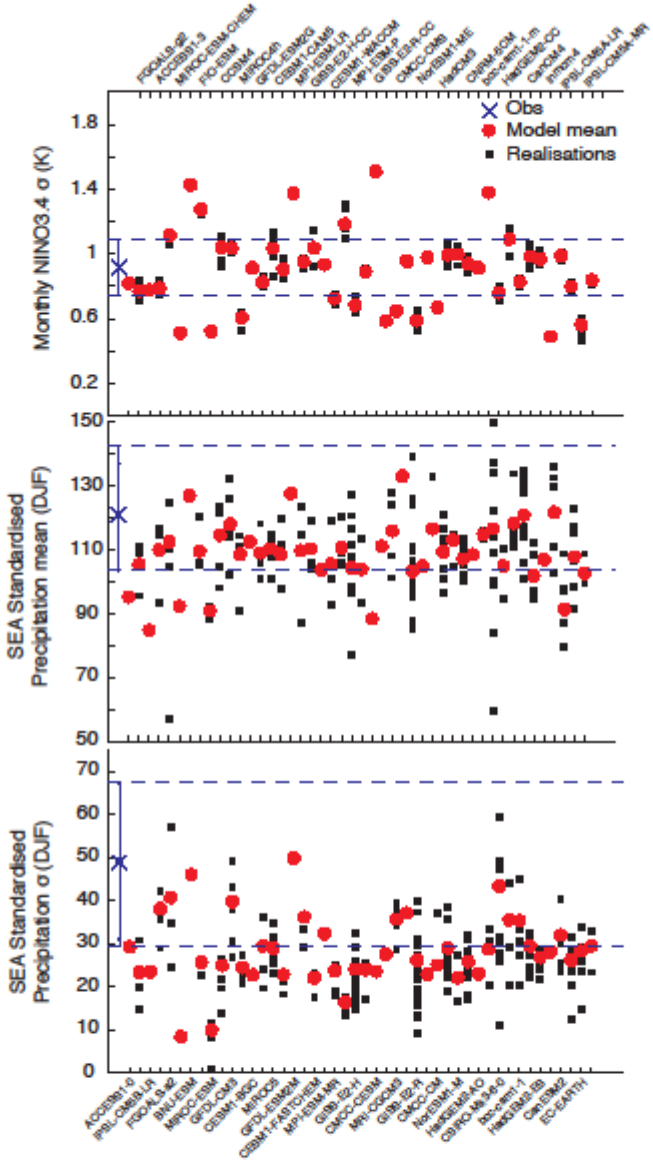

Figure 3
(A) Comparison of observed and simulated NINO3.4 monthly surface air temperature variability (K) for observations and all CMIP5 models with historical experiments archived on the Australian ESG node. (B) As for panel A but showing southeastern Australian standardised DJF mean precipitation as a percentage of normal rainfall defined by the climatological mean) and (C) southeastern Australian standardised DJF precipitation variability (σ). In all plots, the mean observational value is shown by a cross and the 5th-95th percentile range indicated by horizontal dashed lines, as determined by bootstrap resampling observed values. Individual model realisations are shown by black squares and each model mean by red circles. Only models lying within the synthesised observed range for the three performance criteria are

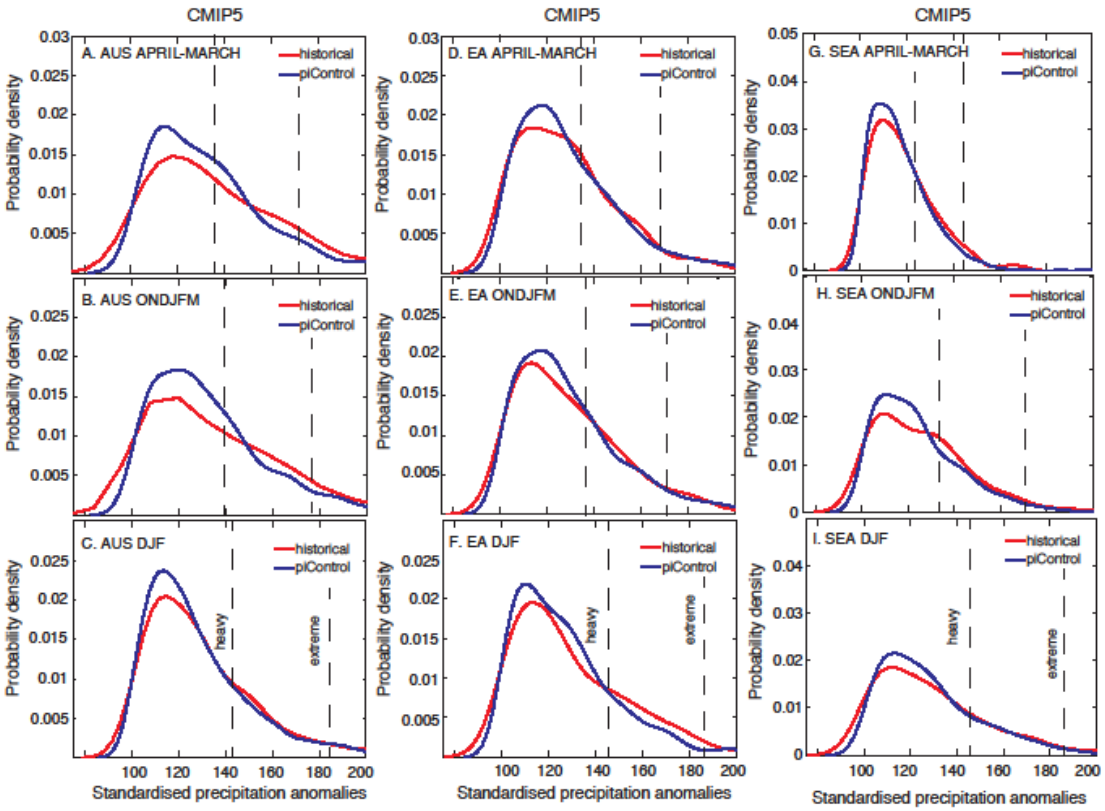

Figure 4.
PDFs for CMIP5 historical (red, 1976-2005 only) and piControl (dark blue, all years shown relative to long-term mean) simulations for Australia (A-C), eastern Australia (D-F) and southeastern Australia (G-H) regions for April-March, ONDFM and DJF seasonal average standardised precipitation (as a percentage of normal rainfall as defined by the climatological mean) for above average rainfall in simulated La Niña years (NINO3.4 SAT anomalies were less than 0.5°C for at least six consecutive months during the year from April to March). Vertical dashed lines show thresholds for one ("heavy") and two standard ("extreme") deviations above climatological mean determined from AWAP observational data for years 1910-2012. The thresholds are based on observed rainfall under all ENSO conditions, so they appear in the dry tail of the distribution of above average simulated rainfall associated with La Niña years.

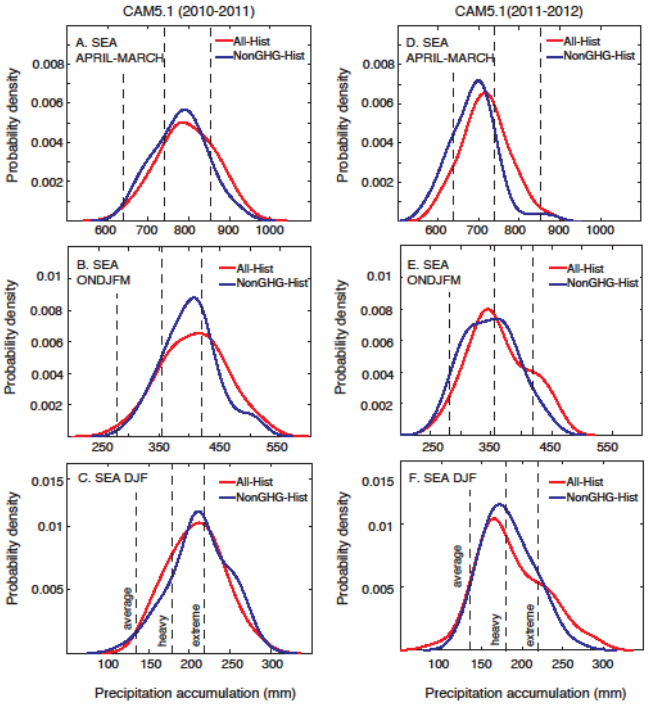

Fiigure 5
PDFs for CAM5.1 All-Hist (red) and NonGHG-Hist (dark blue) simulations for southeastern Australian April-March, ONDFM and DJF seasonal rainfall accumulations (mm) for 2010-2011 (left) and 2011-2012 (right). Vertical dashed lines show thresholds for mean accumulated precipitation (mm) ("average"), one ("heavy") and two standard ("extreme") deviations above climatological mean determined from AWAP observational data for years 1910-2012. As thresholds are determined using rainfall in all observed years, they appear in the dry tail of the rainfall distributions associated with the La Niña years of 2010-2012.

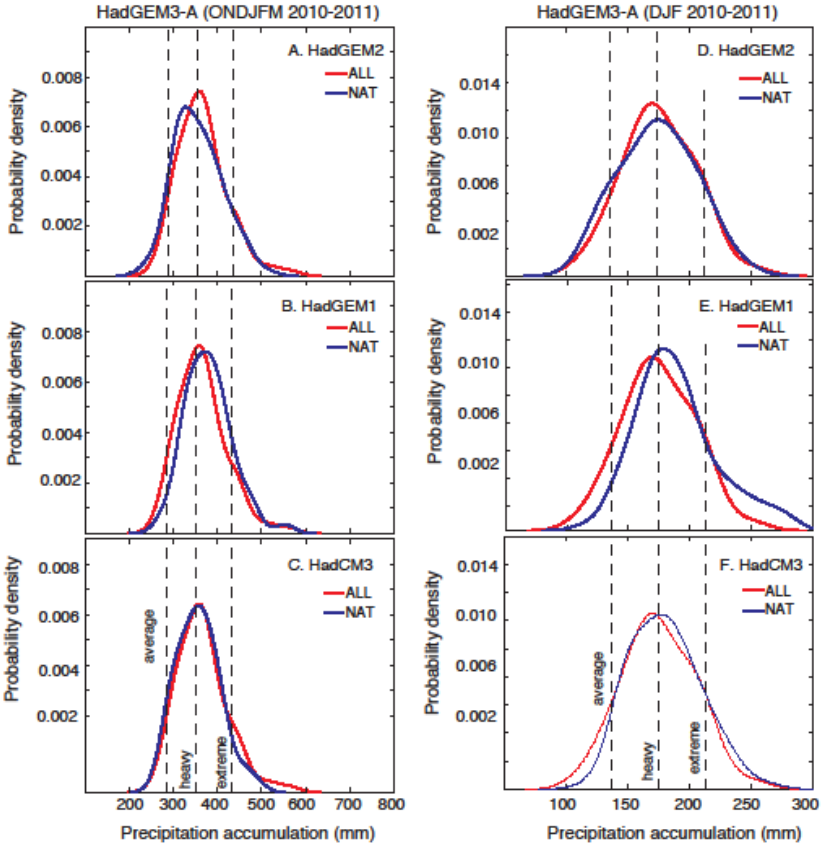

Figure 6
PDFs for HadGEM3-A ALL (red) and NAT (dark blue) simulations southeastern Australia region for ONDFM (left) and DJF (right) seasonal rainfall accumulations (mm) for 2010-2011. Vertical dashed lines show thresholds for mean accumulated precipitation (mm) ("average"), one ("heavy") and two standard ("extreme") deviations above climatological mean determined from AWAP observational data for years 1910-2012. As thresholds are determined using rainfall in all observed years, they appear in the dry tail of the rainfall distributions associated with the La Niña years of 2010-2012.

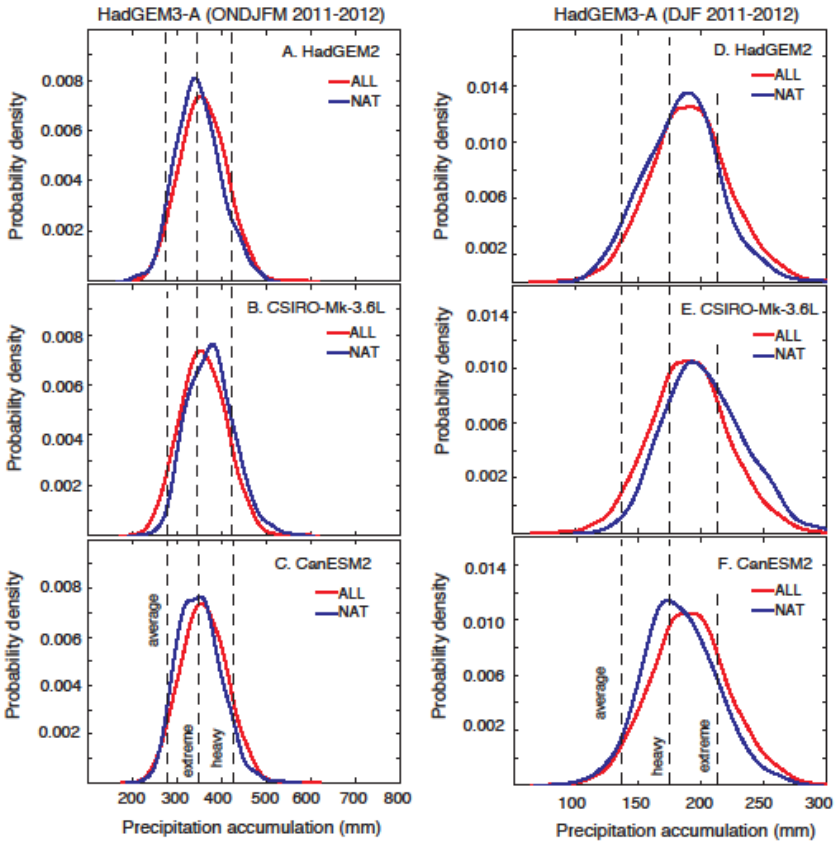

Figure 7
As for Figure 6 but showing 2011-2012 ONDJFM (left) and DJF (right) seasonal rainfall accumulations (mm).

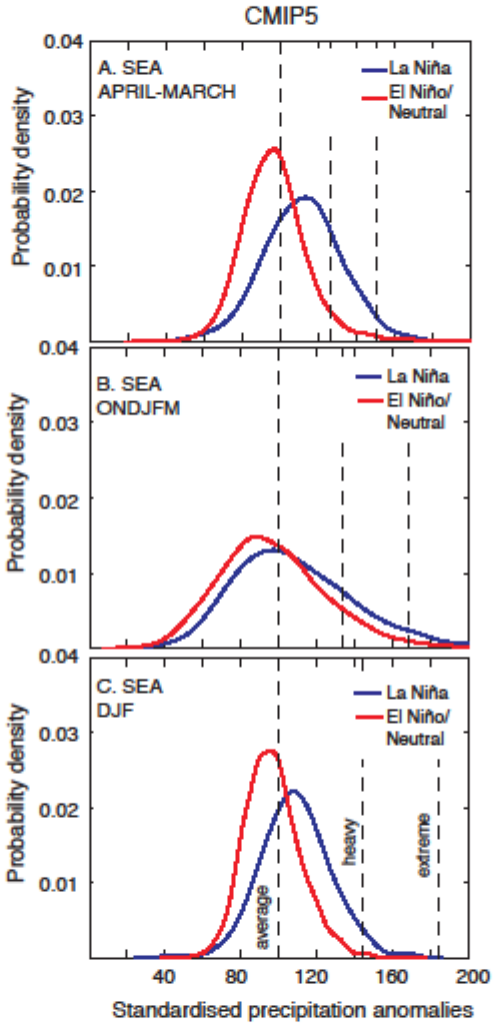

Figure 8
PDFs comparing southeastern Australian standardised rainfall during La Niña (dark blue) conditions derived from CMIP5 historical simulations, with El Niño/neutral (red) conditions. Probability densities are shown for April to March (A), ONDFM (B) and DJF (C) rainfall anomalies. La Niña years are defined where simulated NINO3.4 SAT anomalies were less than 0.5°C for at least six consecutive months during the year from April to March. Vertical dashed lines show thresholds for mean standardised precipitation ("average"), one ("heavy") and two standard ("extreme") deviations above climatological mean determined from AWAP observational data for years 1910-2012.

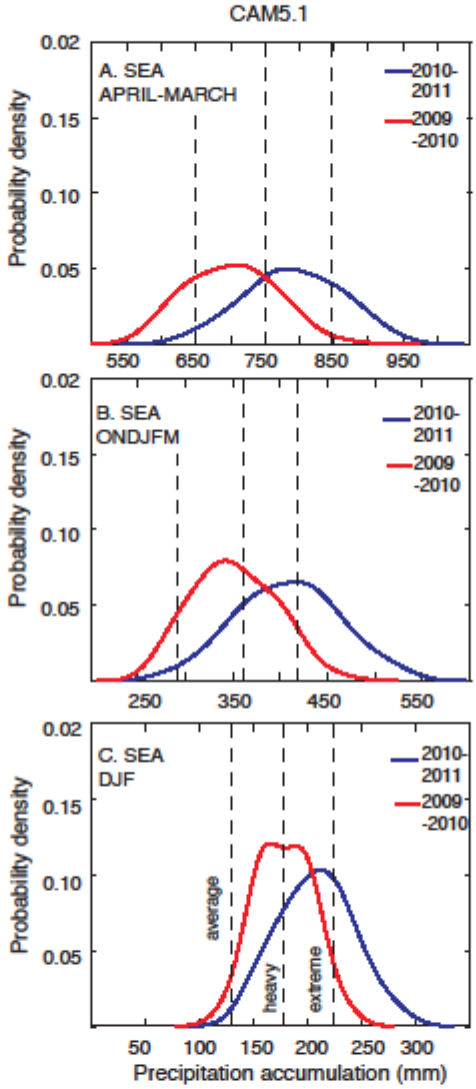

Figure 9.
PDFs for CAM5.1 All-Hist simulations comparing southeastern Australian rainfall accumulations (mm) for 2010-2011 (dark blue) and 2009-2010 (red) conditions. Probability densities are shown for April to March (A), ONDFM (B) and DJF (C). Vertical dashed lines show thresholds for mean accumulated precipitation (mm) ("average"), one ("heavy") and two standard ("extreme") deviations above climatological mean determined from AWAP observational data for years 1910-2012.

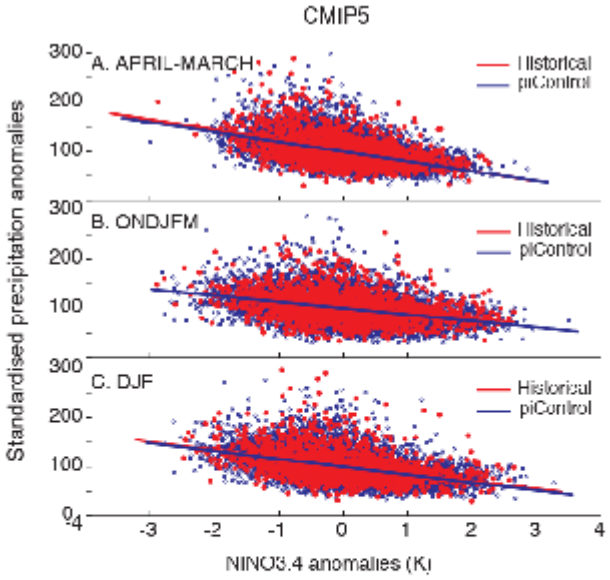

Figure 10
Scatter plots of NINO3.4 surface air temperature anomalies (K) against area-average south-eastern Australian standardised precipitation anomalies for (A) April to March, (B) ONDJFM and (C) DJF for historical (red) and piControl (blue) model years. Lines of best fit are also shown, calculated using ordinary least squares regression.

Table 1

Dataset	Experiments	Description	Model years	Number of simulations	Ensemble	Temperature anomaly baseline	Precipitation anomaly baseline
CMIP5	historicalNat	Solar, volcanics	1850-2005	29	16 models	1850-1900	1850-1900
	historical	Anthropogenic (greenhouse gases,aerosols, ozone) and natural (solar, volcanics)	1976-2005	65	16 models	30-year running mean	1850-1900
	RCP8.5	Anthropogenic (greenhouse gases, aerosols, ozone scenarios) and natural (solar)	2006-2020	45	16 models	2006-2020	1850-1900
	piControl	Non-evolving pre-industrial forcings	All	16	16 models	Long term mean	Long term mean
CAM5.1	All-Hist	Evolving ocean surface temperatures, greenhouse gas concentrations, and aerosol concentrations over the last 50 years	2010,2011,2012	50	Perturbed initial conditions		

	NonGHG-Hist	Greenhouse gas concentrations maintained at pre-industrial levels, with estimates of anthropogenic SST warming removed	2010,2011,2012	50	Perturbed initial conditions
HadGEM3-A	ALL	Evolving ocean surface temperatures, greenhouse gas concentrations, and aerosol concentrations over the last 50 years	2010,2011,2012	99 (2010,2011) and 594 (2012)	Perturbed physics and initial conditions
	NAT	Greenhouse gas and aerosol concentrations maintained at pre-industrial levels, with estimates of anthropogenic SST warming removed	2010,2011,2012	297 (2010,2011) and 1584 (2012)	Perturbed physics and initial conditions

Tab 2

Dataset	Experiments	Models
CMIP5	All experiments	FGOALS-g2
		IPSL-CM5B-LR
		CCSM4
		MPI-ESM-LR
		CESM1-FASTCHEM
		MPI-ESM-P
		HadCM3
		NorESM1-M
		CNRM-CM5
		HadGEM2-AO
		CSIRO-Mk3-6-0
		HadGEM2-CC
		HadGEM2-ES
		CanESM2
		IPSL-CM5A-LR
		IPSL-CM5A-MR
HadGEM3-A	ALL	HadGEM3-A
	NAT (2010, 2011)	HadCM3
		HadGEM1
		HadGEM2

NAT (2012)	CSIRO-MK3-6L
	CanESM2
	HadGEM2